Check for updates

Aberration fields of off-axis astronomical telescopes induced by rotational misalignments

GUOHAO JU,[1] HONGCAI MA,[1,2] AND CHANGXIANG YAN[1,3]

[1]*Changchun Institute of Optics, Fine Mechanics and Physics, Chinese Academy of Sciences, Changchun, Jilin 130033, China*
[2]*hongcma@hotmail.com*
[3]*yancx@ciomp.ac.cn*

Abstract: Due to the absence of rotational symmetry, off-axis astronomical telescopes with off-set pupil become subject to rotational misalignments. Rotational misalignments of large off-axis mirrors with reference to their geometric center can greatly degrade the imaging quality. This paper presents an in-depth discussion on the net aberration fields of off-axis astronomical telescopes induced by rotational misalignments. Aberration function of off-axis telescopes with rotational misalignments is derived based on the framework of nodal aberration theory. Expressions of several important aberrations are obtained under some approximations. Then the specific field characteristics of these aberrations are presented and explicated. Meanwhile, we demonstrate that rotational misalignments can be converted to a kind of surface decenters; on the other hand, the effects of rotational misalignments have their special features which are different from the effects of general surface decenters. Besides, some other insightful discussions are further presented. This work is also applicable to the rotational misalignments of the off-axis segments of primary mirror in segmented mirror astronomical telescopes.

References

1. R. J. R. Kuhn and S. L. Hawley, "Some astronomical performance advantages of off-axis telescopes," Publ. Astron. Soc. Pac. **111**(759), 601–620 (1999).
2. M. Bartelmann and P. Schneider, "Weak gravitational lensing," Phys. Rep. **340**(4–5), 291–472 (2001).
3. F. Zeng, X. Zhang, J. Zhang, G. Shi, and H. Wu, "Optics ellipticity performance of an unobscured off-axis space telescope," Opt. Express **22**(21), 25277–25285 (2014).
4. W. Cao and N. Gorceix, *et al.*, "First Light of the 1.6 meter off-axis New Solar Telescope at Big Bear Solar Observatory," Proc. SPIE **7333**, 73330 (2010).
5. G. Moretto and J. R. Kuhn, "Optical performance of the 6.5-m off-axis New Planetary Telescope," Appl. Opt. **39**(16), 2782–2789 (2000).
6. H. M. Martin, R. G. Allen, J. H. Burge, D. W. Kim, J. S. Kingsley, M. T. Tuell, S. C. West, C. Zhao, and T. Zobrist, "Fabrication and testing of the first 8.4-m off-axis segment for the Giant Magellan Telescope," Proc. SPIE **7339**, 73390A (2010).
7. S. C. West, J. H. Burge, B. Cuerden, W. Davison, J. Hagen, H. M. Martin, M. T. Tuell, C. Zhao, and T. Zobrist, "Alignment and use of the optical test for the 8.4-m off-axis primary mirrors of the Giant Magellan Telescope," Proc. SPIE **7339**, 73390N (2010).
8. J. Matt, J. P. Roger, S. A. Shectman, R. Bernstein, D. G. Fabricant, P. McCarthy, and M. Phillips, "Status of the Giant Magellan Telescope (GMT) project," Proc. SPIE **5489**, 441–453 (2004).
9. M. Clampin, "Status of the James Webb Space Telescope observatory," Proc. SPIE **8442**, 84422A (2012).
10. M. A. Lundgren and W. L. Wolfe, "Alignment of a three-mirror off-axis telescope by reverse optimization," Opt. Eng. **30**(3), 307–311 (1991).
11. H. Lee, G. B. Dalton, I. A. J. Tosh, and S.-W. Kim, "Computer-guided alignment II :Optical system alignment using differential wavefront sampling," Opt. Express **15**(23), 15424–15437 (2007).
12. R. Upton and T. Rimmele, "Active reconstruction and alignment strategies for the Advanced Technology Solar Telescope," Proc. SPIE **7793**, 77930E (2010).
13. R. V. Shack and K. P. Thompson, "Influence of alignment errors of a telescope system," Proc. SPIE **251**, 146–153 (1980).

14. K. P. Thompson, "Aberration fields in tilted and decentered optical systems," Ph.D. dissertation (University of Arizona, Tucson, Arizona, 1980).
15. K. Thompson, "Description of the third-order optical aberrations of near-circular pupil optical systems without symmetry," J. Opt. Soc. Am. A **22**(7), 1389–1401 (2005).
16. K. P. Thompson, "Multinodal fifth-order optical aberrations of optical systems without rotational symmetry: spherical aberration," J. Opt. Soc. Am. A **26**(5), 1090–1100 (2009).
17. K. P. Thompson, "Multinodal fifth-order optical aberrations of optical systems without rotational symmetry: the comatic aberrations," J. Opt. Soc. Am. A **27**(6), 1490–1504 (2010).
18. K. P. Thompson, "Multinodal fifth-order optical aberrations of optical systems without rotational symmetry: the astigmatic aberrations," J. Opt. Soc. Am. A **28**(5), 821–836 (2011).
19. T. Schmid, K. P. Thompson, and J. P. Rolland, "Misalignment-induced nodal aberration fields in two-mirror astronomical telescopes," Appl. Opt. **49**(16), D131–D144 (2010).
20. K. P. Thompson, T. Schmid, and J. P. Rolland, "The misalignment induced aberrations of TMA telescopes," Opt. Express **16**(25), 20345–20353 (2008).
21. J. M. Sasian, "Imagery of the Bilateral Symmetric Optical System," Ph.D. dissertation (University of Arizona, Tucson, Arizona, 1988).
22. T. Schmid, J. P. Rolland, A. Rakich, and K. P. Thompson, "Separation of the effects of astigmatic figure error from misalignments using Nodal Aberration Theory (NAT)," Opt. Express **18**(16), 17433–17447 (2010).
23. K. Fuerschbach, J. P. Rolland, and K. P. Thompson, "Extending nodal aberration theory to include mount-induced aberrations with application to freeform surfaces," Opt. Express **20**(18), 20139–20155 (2012).
24. K. Fuerschbach, J. P. Rolland, and K. P. Thompson, "Theory of aberration fields for general optical systems with freeform surfaces," Opt. Express **22**(22), 26585–26606 (2014).
25. N. Zhao, J. C. Papa, K. Fuerschbach, Y. Qiao, K. P. Thompson, and J. P. Rolland, "Experimental investigation in nodal aberration theory (NAT) with a customized Ritchey-Chrétien system: third-order coma," Opt. Express **26**(7), 8729–8743 (2018).
26. G. Ju, C. Yan, Z. Gu, and H. Ma, "Aberration fields of off-axis two-mirror astronomical telescopes induced by lateral misalignments," Opt. Express **24**(21), 24665–24703 (2016).
27. G. Ju, C. Yan, Z. Gu, and H. Ma, "Nonrotationally symmetric aberrations of off-axis two-mirror astronomical telescopes induced by axial misalignments," Appl. Opt. **57**(6), 1399–1409 (2018).
28. K. P. Thompson, T. Schmid, O. Cakmakci, and J. P. Rolland, "Real-ray-based method for locating individual surface aberration field centers in imaging optical systems without rotational symmetry," J. Opt. Soc. Am. A **26**(6), 1503–1517 (2009).
29. G. Moretto, M. P. Langlois, and M. Ferrari, "Suitable off-axis space-based telescope designs," Proc. SPIE **5487**(163), 1111–1118 (2004).
30. Z. Gu, C. Yan, and Y. Wang, "Alignment of a three-mirror anastigmatic telescope using nodal aberration theory," Opt. Express **23**(19), 25182–25201 (2015).

1. Introduction

Compared to rotationally symmetric on-axis astronomical telescopes with pupil obstruction, off-axis telescopes with offset pupil have many advantages in astronomical observation, such as lower scattering property, larger emissivity throughput, and higher dynamic range [1]. Besides, unobscured off-axis telescopes also have simpler and sharper diffraction pattern, meaning not only higher resolution but also some advantages in ellipticity performance [2], which is of cardinal importance for weak gravitational lensing measurement [3]. While off-axis telescopes have been widely applied in the area of remote sensing, to date only few large off-axis astronomical telescopes have been constructed [4,5]. Apart from the fabrication of large off-axis surfaces, another main challenge that hinders the construction of large off-axis astronomical telescopes lies in the fine alignment as well as active optical compensation and alignment of this class of telescopes [6,7]. Due to the absence of rotational symmetry, the effects of misalignments in off-axis telescopes become more complicated. It is of great significance to illuminate the effects of different kinds of misalignments on the net aberration fields of off-axis astronomical telescopes.

Segmented or synthetic-aperture primary mirrors are efficient solutions to the problems with monolithic primary mirror manufacture and testing, transportation and launch [8,9]. In fact, segmented mirror telescopes and synthetic-aperture telescopes can be seen as an array of off-axis telescopes. Each off-axis segment (or each sub-aperture) of the primary mirror and secondary mirrors compose an off-axis telescope. While the aperture size of each off-axis segment is comparatively small, the magnitude of aperture offset with respect to optical axis can be very large, which can greatly increase the sensitivity of segments to misalignments. In

the alignment of off-axis segments, the insights of the aberrational effects of segment misalignments can help diagnose the misalignment states of the segments and thus facilitate the whole alignment process.

While numerical methods have been used to calculate the misalignments of off-axis systems [10–12], these methods can hardly contribute to an in-depth understanding of effects of misalignments on net aberration fields; on the other hand, these methods still cannot provide any valuable insights or theoretical guidance for the alignment or active alignment of off-axis systems. Nodal aberration theory (NAT), discovered by Shack [13] and developed by Thompson [14–18], is an analytic tool in studying the aberration behavior of on-axis optical systems which contain misaligned, or intentionally tilted and/or decentered components [19,20]. This theory was first extended to study optical systems with plane symmetry [21]. Then, this theory was extended to analytically express the effects of freeform surfaces on the net aberration fields several years ago [22–24]. Recently, the correctness of nodal aberration theory was verified through experiment with a Ritchey-Chrétien telescope [25]. However, when discussing the effects of misalignments, the traditional nodal aberration theory is only applicable to those optical systems comprised of rotationally symmetric surfaces [22]. In other words, traditional nodal aberration theory is not directly applicable to off-axis systems.

In our previous work, we systematically discussed the effects of lateral misalignments (decenter and tip-tilt of optical surfaces in the lateral direction) and axial misalignments (dislocation of optical surfaces along the axial direction) in off-axis two-mirror astronomical telescopes by extending nodal aberration theory to off-axis telescopes [26,27]. While these works can contribute to a better understanding of the effects of misalignments in off-axis telescopes, they are not enough. There exists another kind of misalignments in off-axis systems, i.e., rotational misalignments. In practice, it is very possible that the location of off-axis mirror is correct while it has some rotational error with respect to its geometric center. On-axis telescopes are immune to this kind of misalignments due to the presence of rotational symmetry. However, rotational symmetry is broken due to pupil offset in off-axis telescopes and only a bilateral symmetry is preserved. Rotational misalignments of large off-axis mirrors can greatly degrade the imaging quality while the effects of them are still not well known, which require further study for better understand.

In this paper, we continue to present an in-depth and systematic discussion on the net aberration fields of off-axis astronomical telescopes induced by rotationally misalignments. This work concentrates on three problems: (1) how to analytically express the effects of rotationally misalignments on the net aberration fields; (2) what special characteristics of the aberration fields that will be induced by rotationally misalignments; (3) what valuable insights or theoretical guidance can be provided by the knowledge of the effects of rotational misalignments in off-axis systems. This work will contribute to a deep understanding of the effects of rotational misalignments on the net aberration fields of off-axis telescopes.

This paper is organized as follows. In Section 2, we derive the aberration function for off-axis astronomical telescopes with rotational misalignments. In Section 3, an off-axis telescope suitable for space application is taken as an example to illustrate the special aberration field characteristics that will be introduced by rotational misalignments. Then we continue to some further discussions in Section 4. In Section 5, we summarize and conclude the paper.

2. Aberration function of off-axis astronomical telescopes with rotational misalignments

In this section, we derive the aberration function of off-axis astronomical telescopes with rotational misalignments. To this end, we first convert this problem to an equivalent case which can be handled by nodal aberration theory. We point out and demonstrate that rotational misalignments can be converted to a kind of decenters which have equivalent effects with rotational misalignments.

2.1 Derivation procedure

Net image plane aberration of rotationally symmetric optical systems consists of the sum of all individual surface contributions, which can be descried by the wave aberration expansion in vector form, given by [15]

$$W = \sum_{j}\sum_{p}^{\infty}\sum_{n}^{\infty}\sum_{m}^{\infty} W_{klmj} \left(\vec{H}\cdot\vec{H} \right)^{p} \left(\vec{\rho}\cdot\vec{\rho} \right)^{n} \left(\vec{H}\cdot\vec{\rho} \right)^{m},\tag{1}$$

where $k = 2p + m$ and $l = 2n + m$, $\vec{H}$ is the normalized field vector and $\vec{\rho}$ is the normalized aperture vector, W_{klmj} denotes the aberration coefficient for a particular aberration type of surface j.

Before deriving the aberration function for off-axis systems with rotational misalignments, we here first introduce the aberration function of a nominal off-axis system, which can be seen as an off-axis portion of a larger rotationally symmetric on-axis system. In the following we call it on-axis parent system. The transformation between the pupil coordinate of the on-axis parent system and the off-axis portion is shown in Fig. 1(a), which can be expressed as

$$\vec{\rho} = b\vec{\rho}\,' + \vec{s},\tag{2}$$

where $\vec{\rho}$ denotes the on-axis pupil vector normalized by the half aperture size of the on-axis parent pupil, $\vec{\rho}\,'$ is the off-axis pupil vector normalized by the half aperture size of the off-axis pupil, $\vec{s}$ represents the location of the off-axis pupil relative to the on-axis parent pupil which is normalized by the half aperture size of the on-axis parent pupil, and b represents the scale factor of the aperture size of the off-axis portion relative to the parent on-axis pupil.
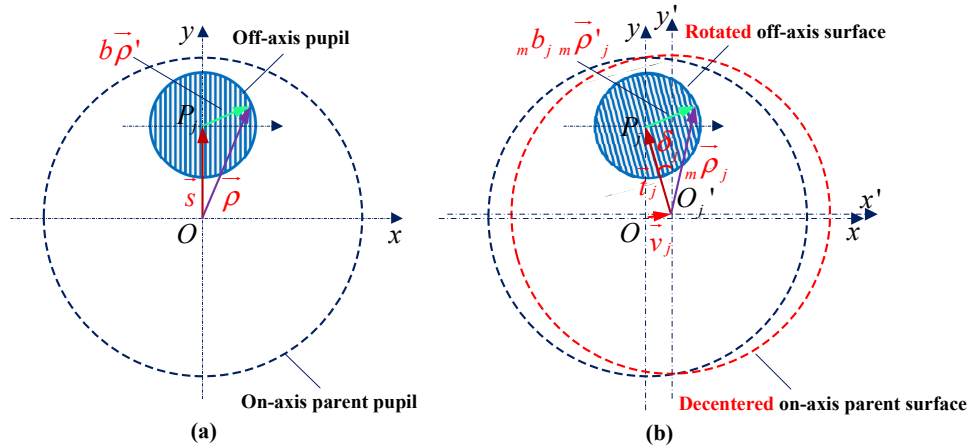

Fig. 1. (a) Coordinate transformation between the pupil of the off-axis system and its rotationally symmetric parent system in the nominal case. (b) Coordinate transformation between the off-axis surface and its rotationally symmetric parent surface when the off-axis surface is rotated about its geometric center.

Then by substituting Eq. (2) into Eq. (1), we can obtain the aberration function of the nominal off-axis system as

$$W = \sum_{j}\sum_{p}^{\infty}\sum_{n}^{\infty}\sum_{m}^{\infty} W_{klmj} \left(\vec{H}\cdot\vec{H} \right)^{p} \left[\left(b\vec{\rho}\,' + \vec{s} \right)\cdot\left(b\vec{\rho}\,' + \vec{s} \right) \right]^{n} \left[\vec{H}\cdot\left(b\vec{\rho}\,' + \vec{s} \right) \right]^{m},\tag{3}$$

where it can be seen that the final measurement is done in the corresponding pupil coordinate of the off-axis system. We can recognize that the aberration function of the off-axis system can be obtained by applying a pupil coordinate transformation to the aberration function of its on-axis parent system. It is important to note that this coordinate transformation is in system level, i.e. aberration contribution of each surface performs the same coordinate transformation.

Now we begin to derive the aberration function of off-axis systems with rotational misalignments. The coordinate transformation between the real off-axis surface with rotational misalignments and its parent surface (which is rotationally symmetric) is shown in Fig. 1(b). We suppose the off-axis surface j is rotated by an angle δ_j with reference to its geometric center, P_j. In this process, the center of its parent surface is translated from O to O_j', and the position of O_j' with reference to O is represented by $\vec{v}_j$ which is normalized by the half aperture size of the parent surface, R_j. The position of P_j with reference to O_j' is represented by $\vec{t}_j$ which is also normalized by half aperture size of the parent surface. $_m\vec{\rho}_j$ is a position vector defined with reference to the center of the on-axis parent surface j normalized by the half aperture size of this surface, $_m\vec{\rho}'_j$ is a position vector defined with reference to the center of the off-axis surface j normalized by the half aperture size of the off-axis surface, and $_mb_j$ is the corresponding scale factor between them. This coordinate transformation describes the relation between the relative positions of the rotated off-axis surface and its parent surface.

We here first reveal some inherent relations between Fig. 1(a) and Fig. 1(b). While Fig. 1(a) illustrates pupil coordinate transformation which is in system level and Fig. 1(b) describes the coordinate transformation in surface level, they become equivalent for the optical surface which serves as the aperture stop. In effect, for the optical surface serving as the aperture stop, the surface level coordinate transformation also determines the system level pupil coordinate transformation. In this case, the magnitude of $\vec{t}_j$ equals to the magnitude of $\vec{s}$ and $_mb_j = b$.

Then we convert the derivation of the aberration function for the off-axis system with rotational misalignments into two separated procedures:

(1) Derive the aberration function for the on-axis parent system with decentered surface.

We can see from Fig. 1(b) that each on-axis parent surface is decentered from O to O_j'. The decenter vector of each surface can be expressed as

$$\vec{V}_j = \begin{bmatrix} S_j \sin\delta_j \\ S_j\left(1-\cos\delta_j\right) \end{bmatrix}, \tag{4}$$

where S_j is the distance from the geometric center of the off-axis surface to the center of the parent surface for surface j. The normalized decenter vector $\vec{v}_j = \vec{V}_j / R_j$, where R_j is the half aperture size of the parent surface.

Since the surfaces in the on-axis parent system are rotationally symmetric, this process can be analytically discussed with nodal aberration theory. Supposing the position of the shifted aberration field center associated with jth decentered surface can be expressed as $\vec{\sigma}_j$, the aberration function of the on-axis parent system can be given by

$$W = \sum_{j}\sum_{p}^{\infty}\sum_{n}^{\infty}\sum_{m}^{\infty} W_{klmj} \left[\left(\vec{H}-\vec{\sigma}_j\right)\cdot\left(\vec{H}-\vec{\sigma}_j\right) \right]^{p} \left(\vec{\rho}\cdot\vec{\rho}\right)^{n} \left[\left(\vec{H}-\vec{\sigma}_j\right)\cdot\vec{\rho} \right]^{m}. \qquad (5)$$

The position of the aberration field center associated with each surface, $\vec{\sigma}_j$, can be analytically calculated with $\vec{V}_j$ and other system parameters [28].

(2) Apply a system level pupil coordinate transformation to the aberration function of the decentered on-axis parent system.

This system level coordinate transformation is determined by off-axis surface which serves as the aperture stop. It may be seen from Fig. 1(b) that the positions of the each off-axis surface with reference to its parent surface are different. However, we should keep in mind that a system has only one exit pupil. The position of this off-axis pupil relative to the on-axis parent pupil is determined by the stop surface. The coordinate transformation between the off-axis pupil and the on-axis parent pupil in this case is expressed as

$$\vec{\rho} = b\vec{\rho}\,' + \vec{t}_0, \qquad (6)$$

where $\vec{t}_0$ specially represents the position of the off-axis surface which serves as the aperture stop with reference to its parent surface and $\vec{t}_0$ has the same magnitude with $\vec{s}$.

On the other hand, the relation between $\vec{s}$ and $\vec{t}_0$ can be expressed as

$$\vec{t}_0 = \vec{s} - \vec{v}_0, \qquad (7)$$

and

$$\left|\vec{v}_0\right| = \left|\vec{s}\right|\left|\delta_0\right|, \qquad (8)$$

where $\vec{v}_0$ specially represents the $\vec{v}_j$ in Fig. 1(b) for the surface which serves as the aperture stop, δ_0 is the rotational error of the off-axis stop surface, and $|\cdot|$ represents the magnitude of a vector or the absolute value of a constant. For misalignment level perturbations, δ_0 is very small (usually $\left|\delta_0\right| < 0.001$). Therefore, we can consider that $\vec{t}_0 = \vec{s}$. In other words, while the parent pupil is decentered, the magnitude of this decenter is so small compared to the magnitude of pupil offset that it nearly does not affect the relative position between the off-axis pupil and the parent pupil.

Then by substituting Eq. (6) into Eq. (5) and considering $\vec{t}_0 = \vec{s}$, we can obtain the aberration function for off-axis systems with rotational misalignments as

$$W = \sum_{j}\sum_{p}^{\infty}\sum_{n}^{\infty}\sum_{m}^{\infty} W_{klmj} \left[\left(\vec{H}-\vec{\sigma}_j\right)\cdot\left(\vec{H}-\vec{\sigma}_j\right) \right]^{p} \left[\left(\vec{\rho}+\vec{s}\right)\cdot\left(\vec{\rho}+\vec{s}\right) \right]^{n} \left[\left(\vec{H}-\vec{\sigma}_j\right)\cdot\left(\vec{\rho}+\vec{s}\right) \right]^{m},$$
$$(9)$$

where for simplicity we assume $b = 1$ (i.e. the off-axis surface has the same aperture size as the on-axis parent surface) and neglect the primes.

Through the above derivation, we can see that the effects of rotational misalignments in off-axis telescopes can be converted to a kind of lateral misalignments which are given by Eq. (4). We can use similar method with reference [26] to expand Eq. (9),

convert the pupil dependence of each term into existing aberration types and group the aberration coefficients according to their pupil dependence. While the field dependence of each aberration type is generally an infinite sum and it is very hard to derive the exact expression for the field dependence of each aberration type, we can obtain some concise expressions that may be not accurate but can provide a direct expression on the aberration field characteristics. When only the third-order aberrations of the on-axis parent system are considered, we can obtain the aberration function of the off-axis system with rotational misalignments as

$$ W = C_{20} \cdot \left(\vec{\rho} \cdot \vec{\rho} \right) + \vec{C}_{22} \cdot \vec{\rho}^{2} + \vec{C}_{31} \cdot \vec{\rho} \left(\vec{\rho} \cdot \vec{\rho} \right) + C_{40} \cdot \left(\vec{\rho} \cdot \vec{\rho} \right)^{2}, \qquad (10) $$

where

$$ C_{20} = W_{020} + \sum_{j} W_{220Mj} \left(\vec{H} - \vec{\sigma}_{j} \right) \cdot \left(\vec{H} - \vec{\sigma}_{j} \right) + 2\sum_{j} W_{131j} \vec{s} \cdot \left(\vec{H} - \vec{\sigma}_{j} \right) + 4W_{040} \left(\vec{s} \cdot \vec{s} \right), (11) $$

$$ \vec{C}_{22} = \frac{1}{2} \sum_{j} W_{222j} \left(\vec{H} - \vec{\sigma}_{j} \right) \left(\vec{H} - \vec{\sigma}_{j} \right) + \sum_{j} W_{131j} \vec{s} \left(\vec{H} - \vec{\sigma}_{j} \right) + 2W_{040} \vec{s}^{2}, \qquad (12) $$

$$ \vec{C}_{31} = \sum_{j} W_{131j} \left(\vec{H} - \vec{\sigma}_{j} \right) + 4W_{040} \vec{s}, \qquad (13) $$

$$ C_{40} = W_{040}. \qquad (14) $$

2.1 Validation for the deviation procedure

In the above subsection, we propose that an off-axis system with rotational misalignments (of each surface) can be seen as a result of selecting a proper off-axis portion of a parent on-axis system in which each surface is decentered. This process can further be interpreted as a decenter of each off-axis surface. The equivalent decenter of each surface is related to the rotational misalignments of each surface, as shown in Eq. (4).

In this subsection, we will perform some suitable simulations to validate this statement. On one hand, we introduce rotational misalignments to an off-axis three-mirror anastigmatic (TMA) telescope. On the other hand, we introduce the corresponding decenter misalignments to each surface which are calculated with Eq. (4). Here an off-axis TMA telescope suitable for space application designed by Gilberto Moretto [29] is used, which was once a preliminary off-axis optical configuration for the Supernova/Acceleration Probe (SNAP) Mission. The aperture size of the primary mirror is 2m and the F number is 10. Optical layout of this telescope is presented in Fig. 2 and the optical design parameters are presented in Appendix A.
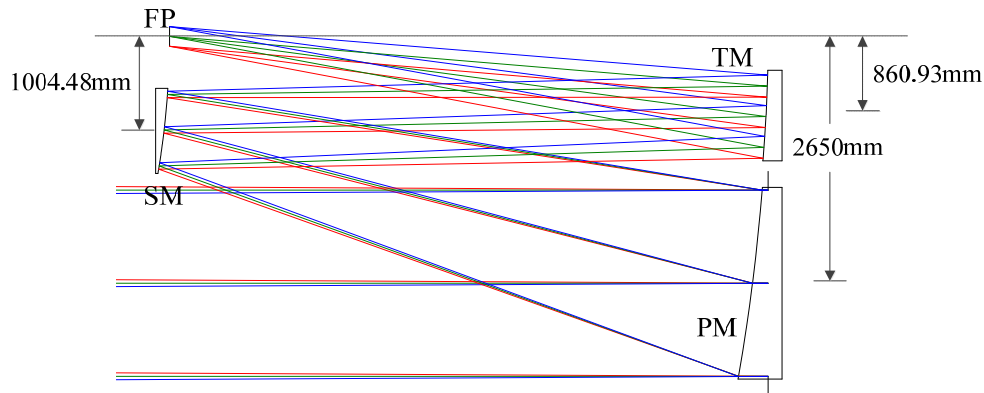
Fig. 2. Optical layout of the off-axis SNAP telescope.

The introduced rotational misalignments of each off-axis surface are shown in Table 1 and the corresponding decenter parameters obtained with Eq. (4) are shown in Table 2, where *XDE* and *YDE* are the vertex decenters of a mirror in the $x-z$ and $y-z$ plane, respectively. The definition for the sign of their directions is in accordance with CODE V. The aberration coefficients of two certain field points, $(0^o, 0^o)$ and $(0.3^o, 0.3^o)$, for the two cases are shown in Table 3. We can see that the aberration coefficients for the two cases are the same with each other. This result can validate the statement that the effects of rotational misalignments are equivalent to the effects of certain surface decenters obtained with Eq. (4).

Therefore, since we have demonstrated the accuracy of the aberration expressions, i.e., Eqs. (10-14), in [26] for off-axis telescopes with lateral misalignments and analyze the deviation between them and the real ray trace data, in this paper we will no longer repeat it and directly use them to analyze the special aberration field characteristics of off-axis telescopes with rotational misalignments.

Table 1. Introduced rotational misalignments

Surface	PM	SM	TM
Rotational error	0.01°	−0.008°	0

Table 2. Equivalent decenters of each mirror obtained with Eq. (4)

Surface	PM	SM	TM
XDE (mm)	−0.4625	0.1403	0
YDE (mm)	−4.036e-05	−9.791e-06	0

Table 3. Fringe Zernike coefficients (2th-9th) for two field points in the presence of the rotational misalignments presented in Table 1 (Case 1) and the decenter misalignments presented in Table 2 (Case 2)

		C2	C3	C4	C5	C6	C7	C8	C9
$(0^o, 0^o)$	Case 1	−0.1988	0.0080	−0.0312	−0.0010	0.8046	−0.0993	0.0034	0.0000
	Case 2	−0.1988	0.0080	−0.0312	−0.0010	0.8047	−0.0993	0.0034	0.0000
$(0.3^o, 0.3^o)$	Case 1	−0.2125	0.0136	−0.0107	0.0098	0.7809	−0.1061	0.0062	−0.0002
	Case 2	−0.2125	0.0136	−0.0107	0.0098	0.7809	−0.1061	0.0062	−0.0002

[a]Fringe Zernike coefficients are in λ ($\lambda = 500$nm

3. Aberration field characteristics of off-axis astronomical telescopes with rotational misalignments

While in the Section 2 we state that rotational misalignments can be converted to a kind of surface decenters in off-axis telescopes, the effects of rotational misalignments have their special features and there are surely differences between the effects of rotational

misalignments and general decenter misalignments. In this section, we will present and explicate the characteristic field dependencies of different aberrations of off-axis astronomical telescopes induced by rotational misalignments. Meanwhile, we mainly focus on the net aberration contribution of rotational misalignments and the interactions between rotational misalignments and nominal aberration can partly be referred to [26] (since rotational misalignments can be converted to special kind of lateral misalignments). We try to provide an intuitive view of the aberration field characteristics induced by rotational misalignments and help grasp the main points.

3.1 Astigmatism

Astigmatism of off-axis astronomical telescopes in the presence of rotational misalignments shown in Eq. (10) and Eq. (12) can be rewritten as

$$W_{AST} = \left(\vec{C}_{22}^{(0)} + \vec{C}_{22}^{(1)} + \vec{C}_{22}^{(2)} \right) \cdot \vec{\rho}^{\,2}, \tag{15}$$

where

$$\vec{C}_{22}^{(0)} = \frac{1}{2} W_{222} \vec{H}^2 + W_{131} \vec{s}\vec{H} + 2 W_{040} \vec{s}^{\,2}, \tag{16}$$

$$\vec{C}_{22}^{(1)} = -\vec{A}_{222} \vec{H} - \vec{A}_{131} \vec{s}, \tag{17}$$

$$\vec{C}_{22}^{(2)} = \sum_j W_{222} \vec{\sigma}_j^{\,2}, \tag{18}$$

and expression of $\vec{A}_{klm}$ is

$$\vec{A}_{klm} = \sum_j W_{klm} \vec{\sigma}_j. \tag{19}$$

Here $\vec{C}_{22}^{(0)}$ represents the astigmatic term of the nominal off-axis system, $\vec{C}_{22}^{(1)}$ represents the astigmatic term that is linearly related to rotational misalignments, and $\vec{C}_{22}^{(2)}$ represents the astigmatic term that is proportional to misalignment squared. When only the net astigmatic aberration contribution of rotational misalignments is considered, we can obtain

$$\Delta W_{AST} = \left(-\vec{A}_{222} \vec{H} - \vec{A}_{131} \vec{s} \right) \cdot \vec{\rho}^{\,2}, \tag{20}$$

where we neglect the astigmatic aberration in the nominal state and that proportional to misalignment squared. We can see that the astigmatism induced by rotational misalignments contains two components, i.e., a field-linear component and field-constant component. Besides, we have also demonstrated in [26] that the magnitude of the field-constant term, $\left| \vec{A}_{131} \vec{s} \right|$, is usually much larger than the magnitude of the field-linear term, $\left| \vec{A}_{222} \right|$ (and therefore there is no astigmatism node in the field of view).

Now we begin to reveal some special features for the astigmatic aberration field induced by rotational misalignments. Considering that the rotational error δ_j is usually very small, the equivalent decenter obtained with Eq. (4) can be rewritten as

$$\vec{V}_j = \begin{bmatrix} S_j \delta_j \\ 0 \end{bmatrix}. \tag{21}$$

We can see that the direction of this equivalent decenter is in x direction, which is perpendicular to the direction of pupil offset. Therefore, the position of the shifted aberration field center associated with each surface, δ_j, is also in the x direction ($+x$ or $-x$ direction).

According to Eq. (19), we can know that the direction of $\vec{A}_{131}$ is in x direction. Therefore, Eq. (20) can be rewritten as

$$\Delta W_{AST} \approx K_{131} \vec{e}_x \vec{s} \cdot \vec{\rho}^{\,2},\tag{22}$$

where we further neglect the small field-linear astigmatic term in Eq. (20) and $\vec{e}_x$ is a unit vector that points to $+x$ direction. $K_{131} = -\left|\vec{A}_{131}\right|$ if the vector $\vec{A}_{131}$ points to $+x$ direction and $K_{131} = \left|\vec{A}_{131}\right|$ if this vector points to $-x$ direction.

Then the direction of the astigmatism induced by rotational misalignments can be approximated as

$$\phi_{AST} = \frac{1}{2}\left[\xi\left(\vec{s}\right) + \xi\left(\vec{e}_x\right) + \psi\left(K_{131}\right)\right],\tag{23}$$

where $\xi(\cdot)$ represents the azimuthal angle of a vector, which is measured from $+x$ axis (and therefore $\xi\left(\vec{e}_x\right) = 0$). $\psi(\cdot)$ can be seen as the azimuthal angle of a constant. $\psi\left(K_{131}\right) = 0$ if $K_{131} > 0$ and $\psi\left(K_{131}\right) = \pi$ if $K_{131} < 0$. The direction of astigmatism is in $[0, \pi)$, and the cycle period is π. If the result of Eq. (23) is not in the range of $[0, \pi)$, we should convert it into this range according to its periodicity.

For the case of the off-axis SNAP telescope shown in Fig. 2, $\xi\left(\vec{s}\right) = 3\pi/2$. According to Eq. (23), we can obtain that the direction of the astigmatism induced by rotational misalignments is roughly $3\pi/4$ or $\pi/4$. Full filed displays (FFDs) provided by CODE V for astigmatism in the off-axis SNAP telescope without and with the rotational misalignments presented in Table 1 are shown in Fig. 3. The length of the line in Fig. 3 represents the magnitude of the astigmatism in certain scale, and the direction of the line represents the direction of the astigmatism. We can see that a large astigmatism which is nearly constant in the field is induced by rotational misalignments. Importantly, we can easily recognize that the direction of this astigmatism is about $\pi/4$.

We can also know that if $\xi\left(\vec{s}\right) = \pi/2$ (in $+y$ direction), the direction of the astigmatism induced by rotational misalignments is still $3\pi/4$ or $\pi/4$. Besides, if $\vec{s}$ is in x direction, i.e. $\xi\left(\vec{s}\right) = 0$ or π, the direction of $\vec{V}_j$ is in the y direction in this case, and therefore the direction of astigmatism is still $3\pi/4$ or $\pi/4$. On the other hand, if the direction of $\vec{s}$ is $3\pi/4$ or $\pi/4$, the direction of the astigmatism induced by rotational misalignments will be 0 or $\pi/2$.

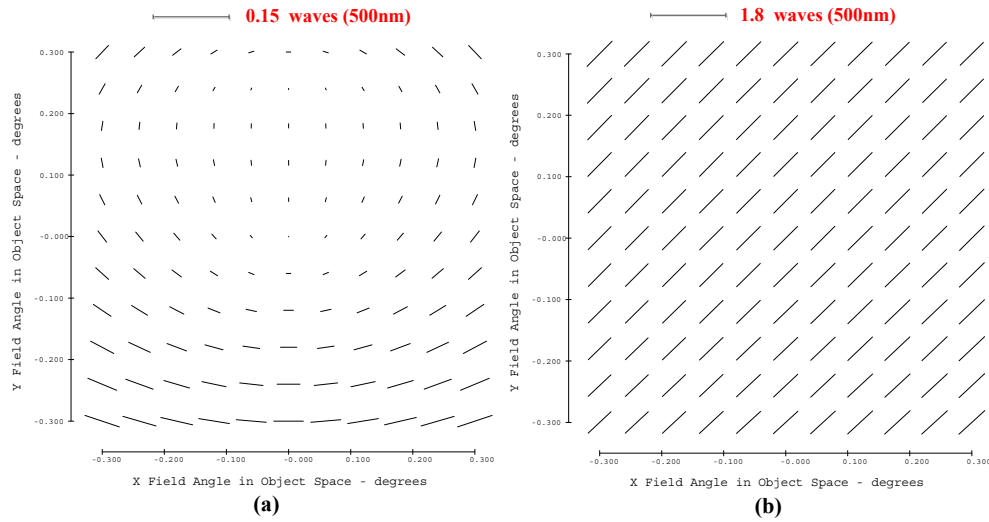0.15 waves (500nm)

1.8 waves (500nm)

Fig. 3. FFDs for astigmatism in the off-axis SNAP telescope (a) without and (b) with the rotational misalignments presented in Table 1. We can see that a large 45° astigmatism which is nearly constant in the field is introduced by rotationally misalignments.

Besides, in on-axis astronomical telescopes, field-constant astigmatism can generally be attributed to astigmatic figure errors. However, in off-axis telescopes, this is not the case. Apart from lateral misalignments, rotational misalignments can also introduce a large field-constant astigmatism. Therefore, it is very hard to separate the effects of astigmatic figure errors between misalignments purely by analyzing astigmatic aberration field.

3.2 Coma

Coma aberration field of off-axis astronomical telescopes in the presence of rotational misalignments shown in Eq. (10) and Eq. (13) can be rewritten as

$$W_{Coma} = \vec{C}_{31}^{(0)} \cdot \vec{\rho} \left(\vec{\rho} \cdot \vec{\rho} \right) + \vec{C}_{31}^{(1)} \cdot \vec{\rho} \left(\vec{\rho} \cdot \vec{\rho} \right), \tag{24}$$

where

$$\vec{C}_{31}^{(0)} = W_{131} \vec{H} + 4W_{040} \vec{s}, \tag{25}$$

$$\vec{C}_{31}^{(1)} = -\vec{A}_{131}. \tag{26}$$

Here $\vec{C}_{31}^{(0)}$ represents the coma term of the nominal off-axis system, which is not affected by misalignments. $\vec{C}_{31}^{(1)}$ represents the coma term that is linearly related to rotational misalignments. The net coma aberration contribution of rotational misalignments can be expressed as

$$\Delta W_{Coma} = -\vec{A}_{131} \cdot \vec{\rho} \left(\vec{\rho} \cdot \vec{\rho} \right). \tag{27}$$

It can be seen that a field-constant coma term will be induced by rotational misalignments. On the other hand, we should also note that the direction of the field-constant coma induced by rotational misalignments is also special. As discussed in the above subsection, the equivalent decenter parameter corresponding to each rotational misalignment obtained with Eq. (4) lies in x direction. Equation (27) can be rewritten as

$$\Delta W_{Coma} = K_{131} \vec{e}_x \cdot \vec{\rho}\left(\vec{\rho} \cdot \vec{\rho}\right). \tag{28}$$

$K_{131} = -\left|\vec{A}_{131}\right|$ if the vector $\vec{A}_{131}$ points to $+x$ direction and $K_{131} = \left|\vec{A}_{131}\right|$ if this vector points to $-x$ direction. Therefore, the direction of the coma induced by rotational misalignments can be expressed as

$$\phi_{Coma} = \xi\left(\vec{e}_x\right) + \psi\left(K_{131}\right). \tag{29}$$

Considering $\xi\left(\vec{e}_x\right) = 0$, the direction of coma is determined by the sign of K_{131} (i.e. the direction of coma is 0 or π).

For the case of the off-axis SNAP telescope shown in Fig. 2, the FFD for coma in the nominal off-axis SNAP telescope is shown in Fig. 4(a), and the FFD for coma in the presence of the rotational misalignments presented in Table 1 are shown in Fig. 4(b). The length of the comet in Fig. 4 indicates the magnitude of coma in certain scale and the head of the comet points to the direction of coma. We can see that a field-constant coma is induced by rotational misalignments. Importantly, we can easily recognize that the direction of this coma is about π.

Direction of the field-constant coma induced by the rotational misalignments is also related to the direction of pupil offset. Specifically, the direction of this coma lies perpendicular to the direction of pupil offset. In other words, if the direction of pupil offset is in x direction, the direction of the coma induced by rotational misalignments will lie in y direction.
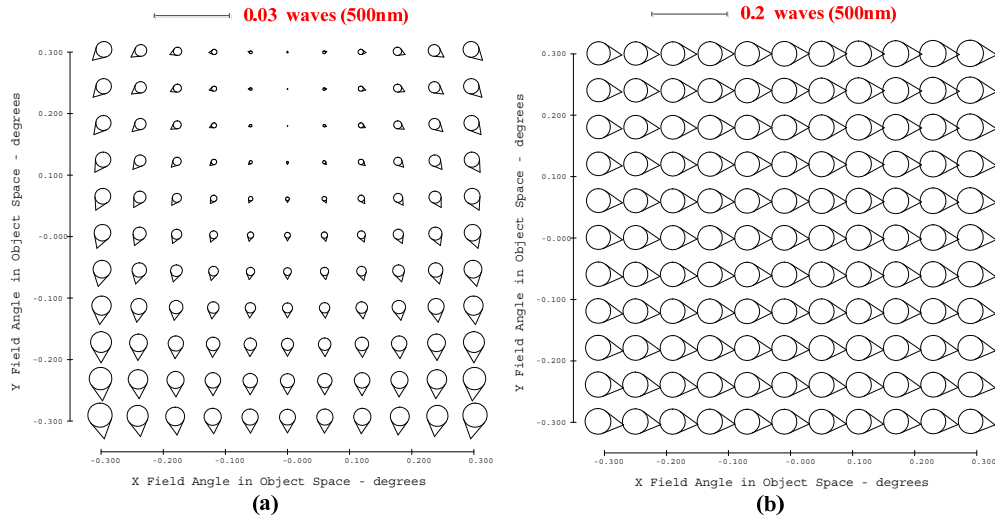

Fig. 4. FFDs for coma in the off-axis SNAP telescope (a) without and (b) with the rotational misalignments presented in Table 1. We can see that a field-constant coma in x direction (perpendicular to the direction of pupil offset) is introduced by rotationally misalignments.

3.3 Medial focal surface

In reference [26] we show that lateral misalignments (decenters and tip-tilts) in off-axis astronomical telescopes can generally introduce a field-constant focal shift. In this paper, we will show that, while rotational misalignments can be converted to a kind of surface decenters, they do not introduce any field-constant focal shift. The reason is that the

equivalent surface decenters corresponding to rotational misalignments obtained with Eq. (4) have a special direction, i.e. they are always perpendicular to the direction of pupil offset.

Medial focal surface of off-axis astronomical telescopes in the presence of rotational misalignments shown in Eq. (10) and Eq. (11) can be rewritten as

$$W_{MFS} = \left(C_{20}^{(0)} + C_{20}^{(1)} + C_{20}^{(2)} \right) \cdot \left(\vec{\rho} \cdot \vec{\rho} \right), \tag{30}$$

where

$$C_{20}^{(0)} = W_{020} + W_{220M} \left(\vec{H} \cdot \vec{H} \right) + 2W_{131} \left(\vec{s} \cdot \vec{H} \right) + 4W_{040} \left(\vec{s} \cdot \vec{s} \right), \tag{31}$$

$$C_{20}^{(1)} = -2\vec{A}_{220M} \cdot \vec{H} - 2\vec{A}_{131} \cdot \vec{s}, \tag{32}$$

$$C_{20}^{(2)} = \sum_j W_{220M} \left(\vec{\sigma}_j \cdot \vec{\sigma}_j \right). \tag{33}$$

Here $\vec{C}_{20}^{(0)}$ represents the medial focus surface of the nominal off-axis system, $\vec{C}_{20}^{(1)}$ represents the medial focus surface that is linearly related to rotational misalignments, and $\vec{C}_{20}^{(2)}$ represents the medial focus surface that is proportional to misalignment squared. The net contribution of rotational misalignments can be given by

$$\Delta W_{MFS} = \left(-2\vec{A}_{220M} \cdot \vec{H} - 2\vec{A}_{131} \cdot \vec{s} \right) \cdot \left(\vec{\rho} \cdot \vec{\rho} \right), \tag{34}$$

where we neglect the term that is proportional to misalignment squared. We can see that the net contribution of rotational misalignments on medial focal surface also contain a field-linear term and a field-constant term. The magnitude of the field-linear term is usually very small and this term has been discussed in reference [15].

Then we continue to discuss the field-constant term. As presented before, the direction of the equivalent decenters of rotational misalignments obtained with Eq. (4) are perpendicular to the direction of pupil offset (which is represented by the direction of $\vec{s}$), and therefore the direction of $\vec{A}_{131}$ is perpendicular to direction of $\vec{s}$, i.e.

$$\vec{A}_{131} \cdot \vec{s} = 0. \tag{35}$$

We can deduce that there is no field-constant focal shift will be induced by rotational misalignments in off-axis telescopes.

FFDs for medial focal surface of the off-axis SNAP telescope in the nominal state and in the presence of rotational misalignments are shown in Fig. 5(a) and Fig. 5(b), respectively. We can hardly recognize the differences between them. On the other hand, FFD for medial focal surface of the off-axis SNAP telescope with some lateral misalignments (not in the direction perpendicular to the direction of pupil offset) is shown in Fig. 5(c), where we can easily recognize a large focal shift. Therefore, while rotational misalignments can be converted to a kind of lateral misalignments, its effects are different from general lateral misalignments in off-axis systems.
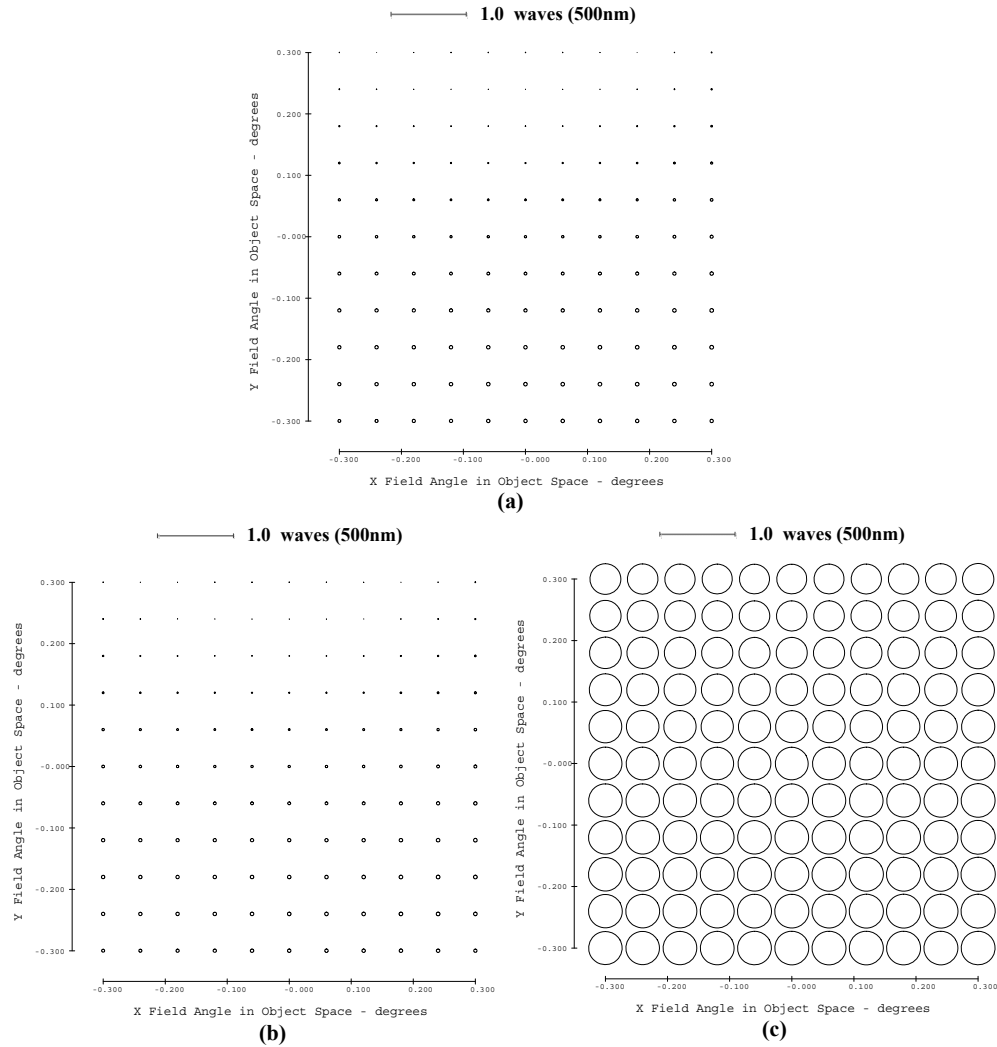
Fig. 5. FFDs for medial focal surface of the off-axis SNAP telescope (a) in the nominal state, (b) in the presence of the rotational misalignments presented in Table 1, and (c) in the presence of some general lateral misalignments (not in the direction perpendicular to the direction of pupil offset). We can see that rotational misalignments do not introduce focal shift while lateral misalignments can generally introduce a large focal shift.

4. Other discussions

In this section, some other brief but insightful discussions concerning the effects of rotational misalignments in off-axis astronomical telescopes will be presented.

4.1 Compensating effects of lateral misalignments to rotational misalignments

In the previous section, we point out that the effects of rotational error of a surface in off-axis telescopes can be seen as a decenter of this surface in the direction perpendicular to pupil offset. In this perspective, we can deduce that while the large off-axis astronomical telescopes are sensitive to rotational misalignments, in practice we do not need to provide adjustable ability to directly correct this kind of misalignments after initial alignment. The effects of rotational misalignments can well be compensated by introducing some proper lateral misalignments (decenters and tip-tilts) to the system.

Here we use a simple example to illustrate the compensating effects of lateral misalignments to rotational misalignments. In the presence of the rotational misalignments presented in Table 1, we can introduce a lateral misalignment of the secondary mirror to compensate for the aberrations induced by rotational misalignments. In practice the secondary mirror is usually smaller in size and weight and it is more convenient to adjust this mirror. The lateral misalignments of the secondary mirror needed for compensation can be computed analytically. Here we take the tertiary mirror as the coordinate reference, i.e., we consider that tertiary mirror is well aligned and the misalignments of the primary mirror and the secondary mirror are defined with reference to the tertiary mirror. In this case, the relationships between the shifted aberration field center for each individual surface and the lateral misalignment parameters can be given by [28] [30]

$$\vec{\sigma}_{PM}^{sph} = \frac{1}{\bar{u}_{PM}} \vec{\beta}_{PM},\tag{36}$$

$$\vec{\sigma}_{SM}^{sph} = \frac{2}{\bar{u}_{PM}} \vec{\beta}_{PM} + \frac{1}{\bar{u}_{PM}(d_1 + r_{SM})}\left(\vec{V}_{PM} - \vec{V}_{SM} - r_{SM}\vec{\beta}_{SM}\right),\tag{37}$$

$$\vec{\sigma}_{TM}^{sph} = \frac{2}{\bar{u}_{PM}} \vec{\beta}_{PM} + \frac{(2d_2 - r_{SM} + 2r_{TM})\vec{V}_{PM} - (2d_2 + 2r_{TM})\left(\vec{V}_{SM} + r_{SM}\vec{\beta}_{SM}\right)}{\bar{u}_{PM}(2d_1 d_2 - d_1 r_{SM} + d_2 r_{SM} + 2d_1 r_{TM} + r_{SM} r_{TM})},\tag{38}$$

$$\vec{\sigma}_{PM}^{asph} = \vec{0},\tag{39}$$

$$\vec{\sigma}_{SM}^{asph} = \frac{1}{d_1 \bar{u}_{PM}}\left(\vec{V}_{PM} - \vec{V}_{SM} + 2d_1\vec{\beta}_{PM}\right),\tag{40}$$

$$\vec{\sigma}_{TM}^{asph} = \frac{2}{\bar{u}_{PM}} \vec{\beta}_{PM} + \frac{(2d_2 - r_{SM})\vec{V}_{PM} - 2d_2\left(\vec{V}_{SM} + r_{SM}\vec{\beta}_{SM}\right)}{\bar{u}_{PM}(2d_1 d_2 - d_1 r_{SM} + d_2 r_{SM})},\tag{41}$$

where $\bar{u}_{PM}$ corresponds to the paraxial chief ray angle at the primary mirror, d_1 is the distance from the primary mirror to secondary mirror, d_2 is the distance from the secondary mirror to tertiary mirror, r_{SM} and r_{TM} corresponds to the radius of the secondary mirror and tertiary mirror, respectively. The up-script *sph* and *asph* indicate that the field center displacement vectors are associated with the spherical base curve and the aspheric departure from the spherical base curve of each individual surface, respectively. $\vec{V}_j$ and $\vec{\beta}_j$ are the vectors representing the magnitude and orientation of the individual surface decenter and tip-tilt parameters, respectively. For the equivalent lateral misalignments corresponding to rotational misalignments of the primary mirror and secondary mirror, we only need to consider surface decenters.

Both the field-constant astigmatism and coma in the off-axis telescope with lateral misalignments are mainly generated from misalignment-induced filed-constant coma of the on-axis parent system through pupil coordinate transformation. Besides, the field-linear astigmatism in off-axis telescope is nearly the same as that in the on-axis parent system. Therefore, the compensating conditions between the equivalent lateral misalignments of rotational misalignments and the lateral misalignments introduced deliberately can be expressed as

$$\begin{cases} \vec{A}_{131} = \vec{0} \\ \vec{A}_{222} = \vec{0} \end{cases}.$$ (42)

The aberration coefficients for each individual surface needed in the calculation are presented in Appendix A. Using Eqs. (36-42), we can obtain the lateral misalignments of the secondary mirror needed for compensating the rotational misalignments in Table 1 (or the equivalent lateral misalignments in Table 2), and the results are $\Delta XDE_{SM} = -0.559$mm and $\Delta BDE_{SM} = -0.00129^{\mathrm{o}}$, where XDE_{SM} and BDE_{SM} represent the vertex decenters and tip-tilts of a mirror in the $x-z$ plane, respectively, and the prefix Δ means these parameters are additionally introduced. Astigmatism and coma aberration fields after compensation are shown in Fig. 6(a) and Fig. 6(b), respectively. Referring to Fig. 3(a) and Fig. 4(a), we can see that both astigmatic and coma aberration field are nearly corrected to their nominal states.
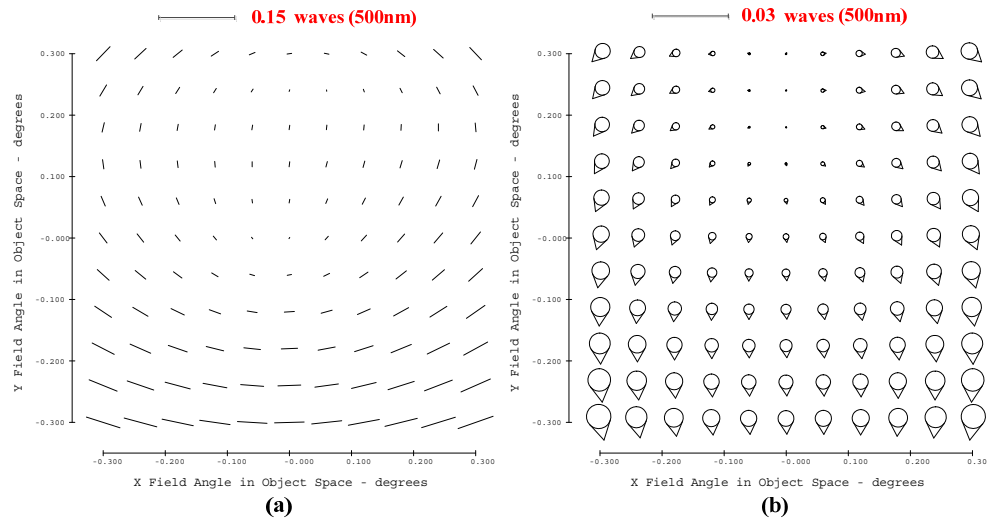

Fig. 6. FFDs for (a) astigmatism and (b) coma in the off-axis SNAP telescope after introducing lateral misalignment of the secondary mirror to compensate for the effects of rotational misalignments presented in Table 1. Referring to Fig. 3(a) and Fig. 4(a), we can see that both the two kinds of aberrations are nearly corrected to the nominal state.

Besides, in the alignment or active alignment of large off-axis telescopes, it is not proper to calculate the lateral misalignments and rotational misalignments at the same time, especially when using sensitivity table method. The sensitivity matrix in this case is ill-conditioned due to the compensating effects between these two kinds of misalignments.

We should also point out that it is not always reasonable to compensate for the effects of rotational misalignments with lateral misalignments. The lateral misalignments needed to compensate for the effects of rotational misalignments may be very large that exceed the adjustable ability of the adjustment mechanism. Therefore, in the initial alignment it is important to guarantee the accuracy of this degree of freedom.

4.2 Magnitude of pupil offset and the sensitivity of astigmatism to rotational misalignments

As shown in Section 3, astigmatism is the dominant aberration in the presence of rotational misalignments. It is of importance to understand the relationship between the sensitivity of astigmatism to rotational misalignments and the magnitude of pupil offset. For example, in the optical design of large off-axis telescopes, we hope that we can select a proper magnitude of pupil offset with which the system is less sensitive to rotational misalignments. For large

segmented mirror astronomical telescopes, different off-axis segments of the primary mirror have different magnitude of pupil offset, and the tolerances of different segments for the rotational errors are different. This subsection discusses the influence of the magnitude of pupil offset on the sensitivity of the astigmatic aberration field to rotational misalignments.

Equation (21) can be rewritten as

$$\vec{V}_j = \begin{bmatrix} \left[\left| \vec{s} \right| R_j{}' \delta_j \right] \\ 0 \end{bmatrix},$$

(43)

where $\left| \vec{s} \right|$ represents the magnitude of $\vec{s}$ and $R_j{}'$ represents the half aperture size of the beam footprint on the surface j (if this surface is the aperture stop, then we have that $R_j{}' = R_j$). We can see that the magnitude of $\vec{V}_j$ is proportional to the magnitude of pupil offset. In other words, the equivalent lateral misalignments corresponding to rotational misalignments are proportional to the magnitude of pupil offset. Considering that the magnitude of $\vec{\sigma}_j$ is linearly correlated with the lateral misalignments of the system, as shown in Eqs. (36-41), the magnitude of $\vec{A}_{131}$ is also proportional to the magnitude of pupil offset. Therefore, the magnitude of $\vec{A}_{131}\vec{s}$, $\left| \vec{A}_{131}\vec{s} \right|$, is proportion to the square of the magnitude of pupil offset. In other word, the sensitivity of astigmatism to rotational misalignments is proportional to the square of the magnitude of pupil offset.

FFD for the astigmatism of the off-axis SNAP telescope with the same rotational misalignments presented in Table 1 with a half magnitude of pupil offset is shown in Fig. 7(a). Comparing the scales shown in Fig. 7(a) and Fig. 3(b), we can see that the magnitude of astigmatism in Fig. 7(a) is only about a quarter of the magnitude of astigmatism in Fig. 3(b).
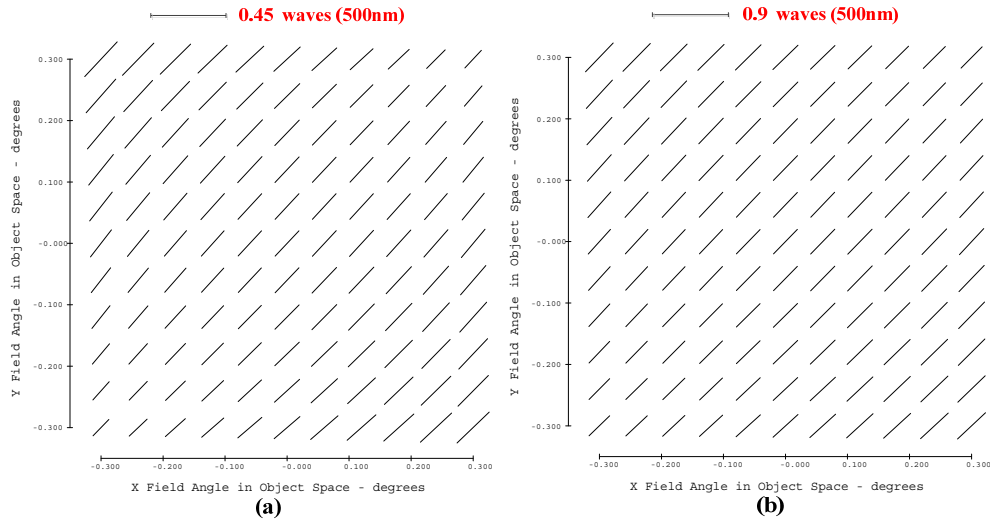

Fig. 7. (a) FFD for astigmatism of the off-axis SNAP telescope with the same rotational misalignments as presented in Table 1while the magnitude of pupil offset is reduced by half (i.e. the distance of the center of the actual primary mirror to the center of its parent surface becomes 1325mm). (b) FFD for astigmatism of the off-axis SNAP telescope with the same misalignments presented in Table 2 while the magnitude of pupil offset is reduced by half.

On the other hand, while rotational misalignments in off-axis systems can be converted to equivalent lateral misalignments, the relationships between the sensitivity of astigmatism to these two kinds of misalignments and the magnitude of pupil offset are different. The

sensitivity of astigmatism to lateral misalignments is linearly related to the magnitude of pupil offset [26]. FFD for astigmatism of the off-axis SNAP telescope with the same lateral misalignments presented in Table 2 while the magnitude of pupil offset is reduced by half is shown in Fig. 7(b), where we can see that the magnitude is half that presented in Fig. 3(b). This is another difference between the effects of rotational misalignments and lateral misalignments.

We can also deduce that the sensitivity of astigmatism to rotational misalignments increases rapidly with the increase in the magnitude of pupil offset. Therefore, in the optical design of off-axis astronomical telescopes, we can reduce the magnitude of pupil offset to reduce the sensitivity of wavefront aberration to rotational misalignments (under the premise that an unobstructed configuration can be obtained). We can also deduce that for large segmented mirror astronomical telescopes, the segments far away from the optical axis are much harder to align than those near the optical axis.

5. Conclusions

This paper extends nodal aberration theory to include the effects of rotational misalignments in off-axis astronomical telescopes and presents a systematic discussion on it. The aberration function of off-axis telescopes with rotational misalignments is derived. The expressions of several important aberrations are obtained under some approximations. Then the specific field characteristics of these aberrations are presented and explicated. Some other insightful discussions concerning the effects of rotational misalignments are also presented.

Some conclusions are presented as follows:

(1) Rotational misalignments can be converted to a kind of surface decenters in off-axis astronomical telescopes. The underlying reasons for this are that each surface in off-axis systems can generally be seen as an off-axis portion of a rotationally symmetric parent surface and rotational errors are usually comparatively small for misalignment level perturbations.

(2) While rotational misalignments can be converted to a kind of surface decenters in off-axis telescopes, the effects of rotational misalignments have their special features and there are differences between the effects of rotational misalignments and general decenter misalignments. Specifically, the directions of astigmatism and coma induced by rotationally misalignment are nearly certain, which are determined by the direction of pupil offset, while directions of astigmatism and coma induced by lateral misalignments can be arbitrary. Besides, rotational misalignments nearly do not affect medial focal surface while lateral misalignments in off-axis telescopes can generally introduce a field-constant focal shift.

(3) Since rotational error of a surface in off-axis telescopes can be seen as a decenter of this surface in the direction perpendicular to pupil offset, the effects of rotational misalignments can well be compensated by introducing some proper lateral misalignments (decenters and tip-tilts) to the system. While large off-axis astronomical telescopes are sensitive to rotational misalignments, in practice we generally do not need to provide adjustable ability to directly correct this kind of misalignments after initial alignment. On the other hand, in general it is not appropriate to compensate for the effects of lateral misalignments by introducing rotational misalignments.

(4) Sensitivity of astigmatism (the dominant aberration induced by rotational misalignments) to rotational misalignments is proportional to the square of the magnitude of pupil offset while of astigmatism to lateral misalignments is linearly related to the magnitude of pupil offset. This fact indicates that as the magnitude of pupil offset increases, the sensitivity of astigmatism to rotational misalignments

increases more rapidly. Therefore, for those off-axis segments (of the segmented primary mirror) far away from the optical axis, we should particularly guarantee the alignment accuracy for this degree of freedom.

Note that not all off-axis astronomical telescopes can be seen as an off-axis portion of an on-axis parent telescope with rotational symmetry. There can be freeform overlays in the nominal design of the off-axis telescope. However, the rotation errors of freeform overlays can easily be handled with a rotating coordinate transformation. We do not further discuss them in this paper.

This work can contribute to a more complete understanding of the effects of misalignments in off-axis astronomical telescopes.

6. Appendix A

Basic optics parameters of the off-axis SNAP telescope are shown in Table 4. Its high-order aspheric parameters are shown in Table 5. The aberration coefficients for the spherical base curve and the aspheric departure from the spherical base curve of each individual surface are shown in Table 6, which are directly obtained from the optical simulation software.

Table 4. Basic optics parameters of the off-axis SNAP telescope

Surface	Radius(mm)	Conic	Thickness(mm)
PM(stop)	−20744.807	−0.9601	−6464.181
SM	−8551.657	0.0000	6464.181
TM	−15497.513	0.0000	−6464.181

Table 5. Aspheric parameters of the off-axis SNAP telescope

Surface	4th-order	6th-order	8th-order	10th-order
PM(stop)	5.286e-15	2.570e-24	0	0
SM	5.197e-13	−1.672e-21	5.704e-29	−2.097e-36
TM	7.093e-14	−5.336e-24	0	0

Table 6. Aberration coefficients for each individual surface

Surface		W_{131}	W_{222}
PM(stop)	Base sphere	−24.3340	2.6432
	Aspheric departure	0	0
SM	Base sphere	15.9805	−2.8066
	Aspheric departure	15.0553	1.3524
TM	Base sphere	−2.1540	0.4052
	Aspheric departure	−4.5546	−1.6750

The aberration coefficients are computed at a field angle of 0.3°, at a wavelength of 0.5 μm.